Results in Physics 10 (2018) 813–817

Contents lists available at ScienceDirect

Results in Physics

journal homepage: www.elsevier.com/locate/rinp

# Transport properties of *Cu-$AlF_3$-W* and *Cu-$AlF_3$-Cu* heterojunctions using STS measurements and a DFT-NEGF approach

J.L. Navarro[a,*], J.C. Moreno-López[d,e], A.E. Candia[a], E.A. Albanesi[a,b], M.C.G. Passeggi Jr[a,c]

[a] Instituto de Física del Litoral (IFIS Litoral-CONICET-UNL), Güemes 3450, 3000 Santa Fe (SF), Argentina
[b] Facultad de Ingeniería, Universidad Nacional de Entre Ríos, 3101 Oro Verde, (ER), Argentina
[c] Departamento de Física, Facultad de Ingeniería Quimica, Universidad Nacional de Litoral, Santa Fe (SF), Argentina
[d] University of Vienna, Faculty of Physics, 1090 Vienna, Austria
[e] School of Physical Sciences and Nanotechnology, Yachay Tech University, 100119-Urcuquí, Ecuador

ARTICLE INFO

*Keywords:*
Electronic transport
Scanning Tunneling Microscopy (STM)
Scanning Tunneling Spectroscopy (STS)
Non Equilibrium Green Functions (NEGF)
$AlF_3$ thin films

ABSTRACT

To understand and to analyze the transport properties of different metal-insulator systems, we developed an experimental study of the electronic transport properties of $AlF_3$ thin films deposited over a *Cu*(1 0 0) substrate, and a theoretical study to model systems composed by an $AlF_3$ molecule between two metallic *Cu*(1 0 0)-*W*(1 0 0) and *Cu*(1 0 0)-*Cu*(1 0 0) electrodes with different geometries. The left common electrode is always a *Cu*(1 0 0) layer, meanwhile the right changing electrode, *W*(1 0 0) or *Cu*(1 0 0), in some cases is represented as a layer and in others as having a tip ending. Tunnelling current against voltage (I-V) characteristic curves have been obtained by Scanning Tunneling Spectroscopy (STS) measurements and computed using density functional theory (DFT) with the non equilibrium Green function method (NEGF) within a bias voltage range from −2.5 to 5.0 V. The theoretical curves show low current values, in the order of $10^{-9}$ to $10^{-12}$, in good agreement with the I-V experimental curves in the same range. This reveals that breakdown response currents begin at higher voltages than 5.0 V. The transmission spectrum, total (DOS) and partial (PDOS) density of states are also presented being the transmission variations addressed in terms of the DOS.

## Introduction

During the last decade, many research groups, theoretical and experimental, have focused on III-VII group insulators compounds and their alloys due to their potential technological applications. The aluminum fluoride ($AlF_3$) is a particular case, which has a great potential in catalysis processes, for instance as a support in reactions between other elements [1,2]; other researchers have reported the use of $AlF_3$ in electron beam lithography as an inorganic resist for nanometer scale patterning [3]; or in electron beam induced decomposition processes for the fabrication of metallic nanowires [4]. Different properties of $AlF_3$, like structural, electronic and optical ones, have been deeply analyzed by many groups in both experimental and theoretical ways. Thereby Konig et al. [5], developed a spectroscopic characterization of different phases of $\alpha$–$AlF_3$, reporting this material as an ionic insulator with a variety of polymorphisms. Chen et al. [6], made a theoretical study using Density Functional Theory (DFT) of the cubic to rhombohedral transition of $\alpha$-$AlF_3$ reporting the total density of states and the dielectric function. Chupas et al. [7], used X-ray diffraction to study the catalytic activity of $AlF_3$, and determined structural changes associated with the extent of the $AlF_6$ octahedra tilting as a function of temperature. Le bail and Calvayrac [8], carried out a theoretical study analyzing the formation of different $AlF_3$ crystal structures by means of a structure prediction computer programme and providing a comparison with ab initio calculations of total energies for the structures, concluding that some crystals would be viable to synthesized. Moreno-López et al. [9], used scanning tunneling microscopy (STM) to investigate the initial growth stages of the interface formed by $AlF_3$ deposited on *Cu*(1 0 0) surfaces at room temperature, while Ruano et al. [10], following those results studied the morphology and thermal stability of $AlF_3$ thin films grown on *Cu*(1 0 0). Daniel et al. [11], studied the structural cubic to rhombohedral transition phase in $AlF_3$ using X-ray diffraction and Raman scattering. Recently, we reported a complete study of different properties of $\alpha$–$AlF_3$ including structural, electronic and optical ones using experimental techniques like electron energy loss spectra (EELS) and X-ray photoelectron spectroscopy (XPS), and performing a theoretical study in the DFT framework including many body effects to increase the accuracy of electronic and optical results,

* Corresponding author.
*E-mail address:* jorge.navarro@santafe-conicet.gov.ar (J.L. Navarro).

https://doi.org/10.1016/j.rinp.2018.07.035
Received 20 April 2018; Received in revised form 27 July 2018; Accepted 29 July 2018
Available online 02 August 2018

through the use of the so called GW approximation theory and the Bethe-Salpeter equation (BSE) [12].

Even so, the charge distribution and electronic transport through an $AlF_3$ solid or molecular layer, settled among metallic electrodes, have not been studied in detail yet. A complete study of transport and electronic properties is important to gain additional insight of the transport properties through an $AlF_3$ layer and know the conditions under which this material could act as an insulator film to support other materials in some devices. The theoretical and experimental information obtained through characteristic I-V curves could be used to improve the efficiency of the systems under study. The state of the art of theoretical tools for charge and electronic transport calculations is a combination between the density functional theory (DFT) and the non equilibrium Green Functions (NEGF) methods, which have been widely used to calculate transport properties of a wide range of nano scale devices.

In this work, we present a theoretical and experimental study of transport properties, including I-V curves, transmission spectra and density of states (DOS), of different interfaces composed by an $AlF_3$ molecule among two metallic electrodes, where the left one is a *Cu* (1 0 0) electrode and the right is a *W*(1 0 0) or *Cu*(1 0 0) electrode with different possible geometries; this is as a structured layer electrode or having a tip-like ending. We report new experimental information about the behavior of $AlF_3$ as an insulator thin film in a voltage range between −10 to 8 V, while by mean of computational calculations we show results between −2.5 to 5 V which are in good agreement with the experimental ones in this range.

## Experimental setup

All STM and STS measurements were performed in an ultra high vacuum (UHV) chamber at room temperature, with a base pressure in the low $10^{-10}$ mbar range. The *Cu*(1 0 0) crystal was cleaned by standard cycles of $Ar^+$ ion bombardment and annealing at 900 K in a reaction UHV chamber attached to the main one. The temperature of the sample was measured at the backside of its holder by means of a chromel-alumel thermocouple.

The aluminum fluoride ($AlF_3$) films were deposited at room temperature in situ over the *Cu*(1 0 0) using a Knudsen cell mounted in the reaction UHV chamber, charged with anhydrous $AlF_3$ (CERAC Inc., Milwaukee, Wisconsin, USA, 99.5%), and heated at 820 K. The cell was carefully degassed until vacuum conditions were in the low $10^{-8}$ mbar during evaporations, and shuttered otherwise to avoid sample contamination. It is worthy to highlight that STM images of clean *Cu*(1 0 0) substrates and $AlF_3$/*Cu*(1 0 0) samples showed no evidence of any contamination after a typical experiment (8–24 h), see [9,10]. The $AlF_3$ deposition rate was between $2 \times 10^2$ and $8 \times 10^4$ ML/s. Tungsten electrochemical etched tips were used for all STM and STS measurements reported in this work. The W polycrystalline tips were routinely cleaned by $Ar^+$ ion bombardment and annealing in UHV. As it is usual for acquiring I-V curves, the feedback loop was turned off during the STS data acquisition. The I-V curves were taken over different points of an atomically flat clean *Cu*(1 0 0) surface and $AlF_3$ islands covering almost completely the copper sample (0.75 ML coverage). The I-V curves shown in this work represent the average of at least 30 reproducible measurements, even changing the measurement point or area and/or the potential sweep rate for each one of the surfaces. The STS curves presented here were measured over a voltage range between −3 and 3 V for the clean copper surface, and −10 and 8 V for the $AlF_3$ islands, using constant initial bias voltage/tunnel currents ($V_{bias}/I_T$) values of 300 mV/0.6 nA and 2500 mV/0.1 nA for the clean copper surface and $AlF_3$ islands, respectively. WS×M free software [13] was used for image acquisition and processing.

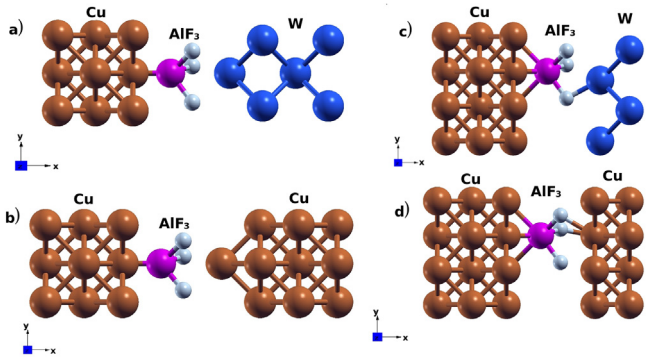


**Fig. 1.** (a) System composed by a *Cu* layer as the left electrode, the $AlF_3$ molecule in between and a set of *W* atoms with a tip-like ending as the right electrode, (b) idem as (a) but with the right electrode composed by *Cu* atoms, (c) system composed by a *Cu* layer as the left electrode, the $AlF_3$ molecule in between and a set of *W* atoms with a layer form as the right electrode, (d) idem as (c) but with the right electrode made of a *Cu* atoms layer.

## Computational details

The calculations reported here, were carried out by means of the software package OpenMX [14]. Fully relativistic norm-conserving pseudo-potentials (PS), and pseudo-atomic orbitals (PAO's) for the expansion of the wave function, contributed by Ozaki and Kino [15,16], were used. The PAO basis functions used for the different elements were *Cu*6.0-s2p2d1, *W*7.0-s3p2d1f1, *Al*7.0-s2p2d1 and *F*5.0-s2p2, respectively. As an example, *W* is the atomic symbol, 7.0 (Bohr) is the cutoff radius specified according to the confinement scheme used [15,16], and s3p2d1f1 represent the number of used orbitals. In this case, there are three primitive *s* orbitals, two for *p* orbitals and one for both *d* and *f* orbitals. For the exchange and correlation potential, we used the Perdew Burke Ernzerhof [17] Generalized Gradient Approximation (GGA).

Also, we used the super cell method to model all systems under study. In total, we worked with four different systems where the electrodes were made by atomic arrangements with a tip-like ending or a layer form of *W* and *Cu*, as shown in Fig. 1(a)–(d). The number of atoms included in each cell depends on the geometry under consideration.

All models were designed to resemble or represent the situation of our STM and STS scanning tunneling microscopy measurements, where a thin film or a molecule is deposited over the substrate, and a tip of tungsten is used to test the transport charge properties. It is important to highlight here that even when we use bulk tungsten tips with edge ending of a few atoms in our experiments, as a part of a standard cleaning procedure, sometimes we crash the tip into the clean copper surface, which means that the possibility of having a copper ended tip cannot be dismissed.

In all our systems we used a molecule of aluminum fluoride ($AlF_3$) among two metallic materials which have the role of representing the substrate (left-lead) and the exploring tip (right-lead). The right-lead is considered in two different geometries, as a layer or a tip, being the last one considered as the most realistic model.

In all systems, the molecule-substrate interface is perpendicular to the *x* axis, while periodic conditions have been maintained in the *yz* plane. For the self consistent calculation, the real space was discretized using a $1 \times 50 \times 25$ Monkhorst [18] k-grid mesh with a cutoff energy of 250 Ry, while electronic densities, density of states (DOS) and transport properties were calculated with the k point meshes shown in Table 1, column 4. The energy convergence for NEGF was considered satisfactory at $1 \times 10^{-4}$ Ha. The interface is modeled with semi-infinite electrodes (replicated ad-infinitum semi-periodically) and a central region including the molecule and some atoms from left and right sides, respectively, in order to have a smooth electronic transition between

**Table 1**
Parameters used for the slab calculations.

| System name | Cell parameters (Å) | Number of atoms | k-grid |
|---|---|---|---|
| *Cu-AlF*$_3$*-W* Tip-lead Fig. 1(a) | $x = 25.9962$ $y = 7.2299$ $z = 7.2299$ | 28 | 1 × 10 × 10 |
| *Cu-AlF*$_3$*-Cu* Tip-lead Fig. 1(b) | $x = 27.3767$ $y = 7.2299$ $z = 7.2299$ | 32 | 1 × 10 × 10 |
| *Cu-AlF*$_3$*-W* Layer-lead Fig. 1(c) | $x = 19.6862$ $y = 7.2299$ $z = 7.2299$ | 36 | 1 × 10 × 10 |
| *Cu-AlF*$_3$*-Cu* Layer-lead Fig. 1(d) | $x = 20.1462$ $y = 10.9048$ $z = 7.2299$ | 44 | 1 × 10 × 10 |

leads and molecule. The $AlF_3$ molecule is located at 1.8 Å from the substrate in the *x* direction, as it was found by Gómez et al. [19], while the electrodes are at a constant distance of 1.8 Å respect to the molecule in the *x* direction.

The different parameters used for each system are summarized in Table 1, where the cell parameters, the number of atoms in each supercell and the k-point meshes used for the NEGF transport calculation are included. Cartoons of all the mentioned models are depicted in Fig. 1.

Quantum conductance properties of the $AlF_3$ molecule placed between two semi-infinite electrodes with different geometries were investigated using a combination between DFT and NEGF method. Electronic transport computations were developed in a bias voltage range between −2.5 V to 5.0 V in step sized intervals of 0.5 V without gate potentials. The transmission spectra and density of states (DOS) are also reported, with the transmission behavior explained in terms of the DOS variations. The left copper electrode is taken as the reference (with electrochemical potential $\mu_L = 0$) and the Fermi energy of the right electrode is shifted by $\mu_R = 1$, 2 and 3 eV, which successively correspond to the bias voltages used in the calculations for V = 1, 2 and 3 V, where $V = \mu_L - \mu_R$.

To calculate the current through the systems, we used the Landauer formula

$$I = \frac{e}{h}\int dE T(E)\Delta f_{RL}(E) \quad (1)$$

where the difference between the Fermi Dirac distribution functions centered at the chemical potentials of the electrodes is represented by $\Delta f_{RL}(E)$, and the transmission $T(E)$ is a k-space integrated expression as obtained within the Green's functions formalism [14].

## Results and discussion

By STS measurements I-V curves were obtained at room temperature by the deposition of 0.75 ML of $AlF_3$ on *Cu*(1 0 0). The results are shown in Fig. 2, where the dashed and dotted lines represent the experimental currents obtained in the experiments and the continuous lines represent the theoretical values obtained through calculations. Whereas the black dashed line represents the tunneling spectra of clean *Cu* (1 0 0), the red dotted line represents the experimental tunneling spectra of the $AlF_3$ islands over *Cu*(1 0 0). Besides, the blue and orange curves correspond to enveloping lines obtained from the theoretically calculated values for the systems with tip-like right electrodes, (blue for *W* and orange for *Cu*, respectively). In Fig. 2, the experimental results show an almost linear response for the clean *Cu*(1 0 0) surface as expected for a material with a metallic behavior. In contrast, tunneling spectra with the tip positioned over $AlF_3$ islands exhibit very low currents ($I < 0.04$ nA) between −5 to 5 V (see the inset of Fig. 2). It is quite evident that theoretical calculations of the most realistic tip-like models *Cu*−$AlF_3$−*W* and *Cu*−$AlF_3$−*Cu* have an excellent agreement with the experimental values in the region between −2.5 to 5 V.

The calculations were performed up to the operational range of interest about 5 V for these interfaces, which in addition is close to the limit in reaching convergence for transport calculations. It is observed that the presence of $AlF_3$ blocks change the electronic charge transmission, acting like an effective insulating region up to the rupture region reached at about the range of 4–5 V.

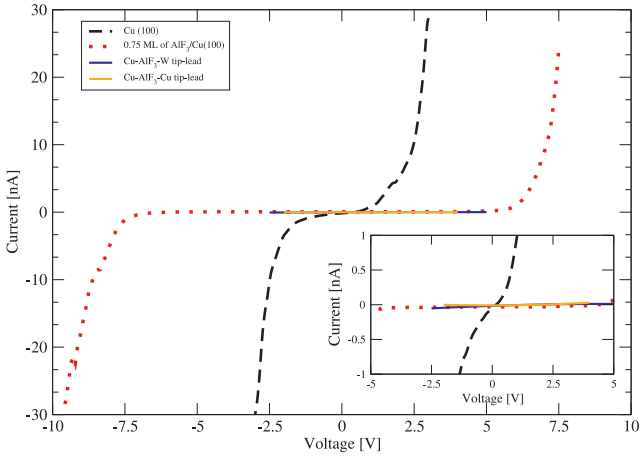


**Fig. 2.** Theoretical I-V curves for systems proposed with a *W* (blue crossed-line) and *Cu* (orange crossed-line) right electrode with a tip-like form, compared to those obtained experimentally for clean *Cu* and $AlF_3$ islands surfaces (black dashed and red dotted lines, respectively). (For interpretation of the references to color in this figure legend, the reader is referred to the web version of this article.)

The coincident experimental and theoretical results allow us to confirm this material as an insulator film to support other materials in some heterostructures.

Fig. 3 shows the DOS obtained for the *Cu-AlF*$_3$*-W* system represented in Fig. 1(a), including the total (DOS) and partial densities of states (PDOS) corresponding to different atoms of the system, a *Cu* atom from the substrate (near the interface between *Cu* and the $AlF_3$ molecule) and another one from the bulk (more internal atoms away from the $AlF_3$ molecule). Also, the *Al* and *F* atoms PDOS are shown, as well as the PDOS corresponding to a *W* atom located in the tip, together with other located in the inner-right electrode. Fig. 3, reveals the energy regions where every element has its main contribution, thus *Cu* states contribute mostly to the edge of the valence band near the Fermi level ($E_f$), while the d-states from *W* contribute to the peaks after $E_f$. The peaks corresponding to energies above the 10 eV region are produced by the 5f-states of *W*. The p-states from *F* atoms are located around −5 eV together with a few bonding p-states from *Al* atoms, while the greatest *Al* contribution appears in the conduction bands at about 10 eV. The *W*

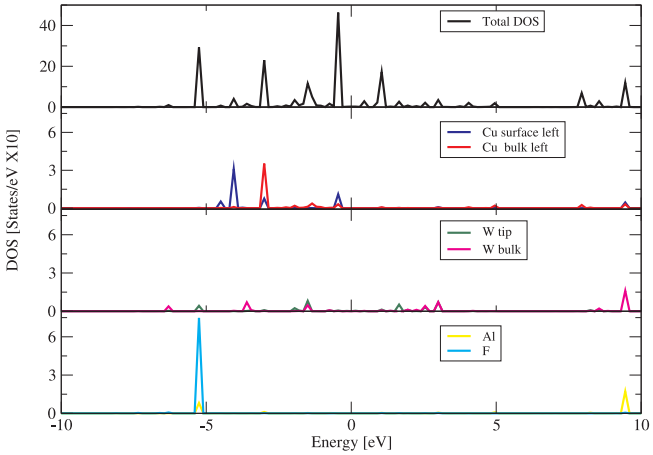


**Fig. 3.** Total and projected DOS computed for the system shown in Fig. 1(a) at 0 V between −10 to 15 eV.

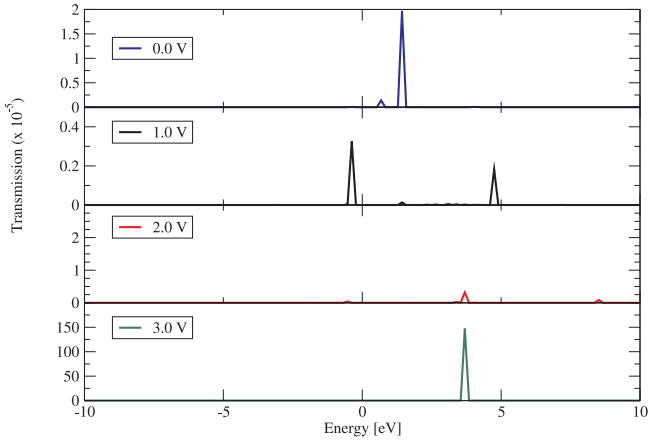


**Fig. 4.** Transmission spectrum of the system depict in Fig. 1(a) at 0, 1, 2 and 3 V bias voltages.

atom located in the tip, has strong contributions above $E_f$ between 0 and 5 eV. The states observed in the DOS between 1.5 and 3.5 eV in Fig. 3 are those states which allows us to measure images and obtain the experimental I-V curves of Fig. 2. However, in the experimental curves no changes in the region between −2.5 and 5 eV are observed because the magnitude of the measured current is very small, in the order of picoamperes, as it was established in the experimental setup.

In Fig. 4, the transmission spectrum of the system represented in Fig. 1(a) calculated at a bias voltages of 0, 1, 2 and 3 V is plotted, showing peaks which are mostly small in magnitude. Here, it is important to notice that $AlF_3$ is an insulator which in bulk, as it was previously reported [12], has a high band-gap of 10.8 eV, which means that a great difference in voltage is needed between left and right electrodes to obtain enough energy to overcome the band-gap existent in these interfaces.

On the other hand, Fig. 5 shows the DOS of the *Cu*-$AlF_3$-*Cu* system with a *Cu* right electrode in a tip-like ending (see Fig. 1(b)), including the PDOS corresponding to atoms located at different places, i.e., an atom of *Cu* located at the tip of the right electrode, other located on the left electrode in the surface near the $AlF_3$ molecule, and two *Cu* atoms considered like bulk atoms located more internally at the left and right electrodes, respectively. We also obtained the PDOS of *Al* and *F* atoms. The total DOS has peaks at −3, −1, 3 and 6 eV, with the main contributions due to the d-states of *Cu*, specially at −1 eV. While the peak at 3 eV is produced by a mixture between s and p-states from *Cu*, the peak at 6 eV is due to contributions mainly of p-states of *Cu* and in a

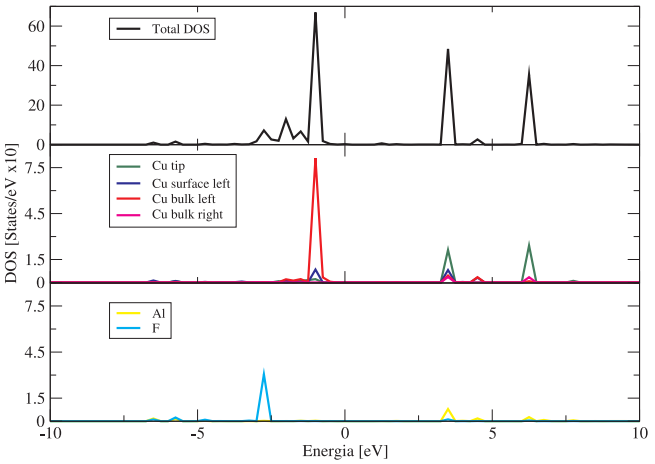


**Fig. 5.** Total and projected DOS computed for the system shown in Fig. 1(b) at 0 V between −10 to 10 eV.

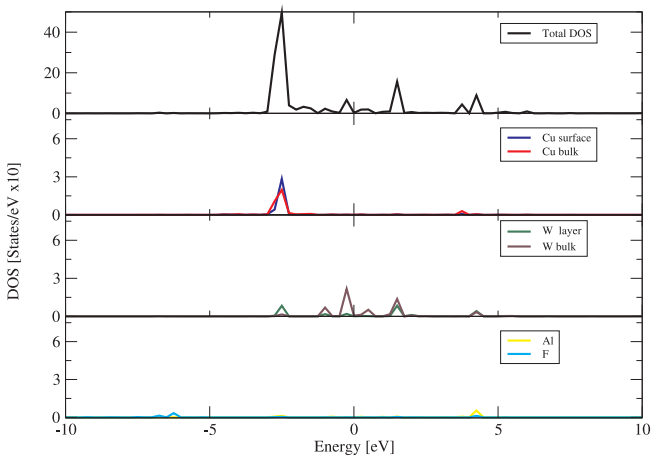


**Fig. 6.** Total and projected DOS computed for the system shown in Fig. 1(c) at 0 V between −10 to 10 eV.

lesser extent from p-states of *Al* atoms.

For the cases with layer-form ending electrodes, shown in Fig. 1(c) and (d), a similar behavior is observed regardless of the material from which the electrode is made. Fig. 6, shows the total and partial DOS for the *Cu*-$AlF_3$-*W* system represented in Fig. 1(c), including total (DOS) and partial densities of states (PDOS) corresponding to a *Cu* atom from the left electrode near the interface between *Cu* and $AlF_3$ molecule and another *Cu* atom considered like a bulk atom from left electrode; also included are the PDOS corresponding to a *W* atom located at the interface of the molecule and the layer and another *W* atom from the bulk (more internal atom away from the molecule). Also, the *Al* and *F* atoms DOS are shown, as well as the PDOS. The total DOS has a main peak located at −2.5 eV due to d-states from *Cu* atoms and small peaks near the Fermi level at −1 eV produced by d-states of the W atoms, which also have important contributions in the energy region of 1.5 eV and beyond. The *Al* atoms have important contributions in the region of 4 eV, while the contribution of the *F* atoms appear mainly as a really small peak at −6 eV.

On the other hand, the calculated transmission spectrum for *Cu*-$AlF_3$-*W* system with a layer form electrode is shown in Fig. 7. These plots represent the transmission probability at bias voltages of 0, 1, 2, 3 and 4 V for the system showed in Fig. 1(c). As it is observed, the peaks have greater intensities for the applied voltages than the transmission spectrum of the *Cu*−$AlF_3$−*W* system with tip-like ending.

In Fig. 8, the DOS and the PDOS at 0 V for the *Cu*-$AlF_3$-*Cu* system represented in Fig. 1(d) with a *Cu* layer-lead right electrode is shown.

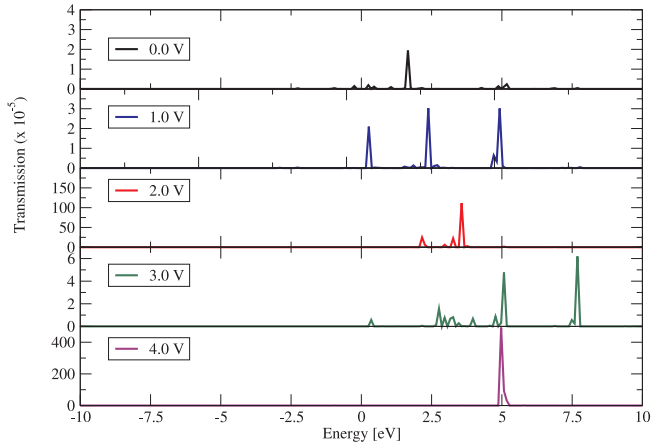


**Fig. 7.** Transmission spectrum of the system depict in Fig. 1(c) at 0, 1, 2, 3, 4 V bias voltages.

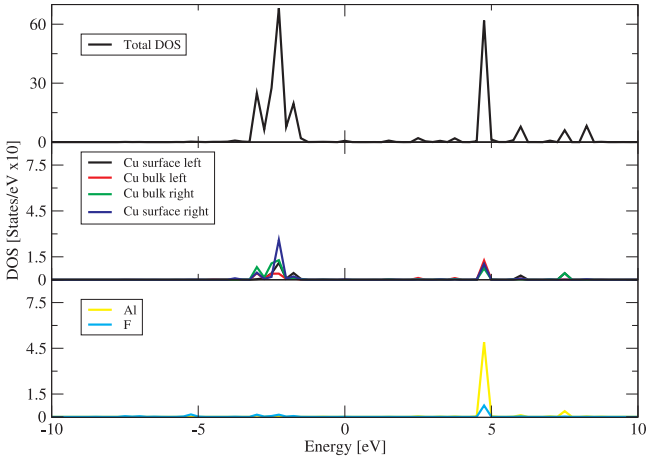


**Fig. 8.** Computed total and partial density of states for the system shown in Fig. 1(d) at 0 V between −10 to 10 eV.

The PDOS corresponding to a *Cu* atom from the left electrode, near the interface between *Cu* and the $AlF_3$ molecule, and to another *Cu* atom considered like a bulk atom from left electrode are included as well as the PDOS corresponding to a *Cu* atom located at the interface between the molecule and the layer (right electrode), and to another *Cu* atom from the bulk (more internal atom away from the molecule). Also, the *Al* and *F* atoms DOS are shown, as well as the PDOS. Clearly the DOS has two main peaks located in energy regions between −3 to −1 eV and 4 to 5 eV, and some other smallest peaks at 6, 7.5 and 8 eV. Looking at the PDOS spectrum, we can observe that peaks from −3 to −1 eV are due to contributions of the d-states from *Cu* atoms, as well as to peaks located between 4 and 5 eV, which in addition present a comparable proportion from *F* atoms and a higher contribution from *Al* ones.

The different plots for the DOS, PDOS and transmission probabilities allow us to understand the relationship between atomic electronic states, it's energy and applied bias voltages. From the analysis of these results, it is clear that the presence of allowed states in the region between −2 to 5 eV makes possible the measurement of the I-V curve over $AlF_3$ islands, although the magnitude of the resulting currents are very small. Comparing the DOS and transmission probabilities, we can observe that these small currents observed are in agreement with the low transmission probabilities that an electron will travel from the left to right electrode, as it observed in Figs. 4 and 7, confirming the insulator behavior of the material for this range of voltages. In this work, a more complete analysis of the tungsten electrode systems was done, considering that they are closer to what we believe occurs during an experimental situation.

## Conclusion

Experimental measurements were used to obtain the I-V curves for a system composed by a film of 0.75 ML of $AlF_3$ deposited over *Cu*(1 0 0) at room temperature. A linear function of the current I(V) curves for the clean *Cu*(1 0 0) surface is observed, a metallic behavior as expected for *Cu*. On the other hand, measurements of the tunneling spectra with the tip positioned over the $AlF_3$ islands exhibit very low current ($I < 0.04$ nA) over the working range of interest. These experimental results were compared with modeling ones using a DFT + NEGF method to calculate the electron transport on some proposed devices composed by an $AlF_3$ molecule between two electrodes with different geometries in a range of bias voltages from −2 to 5 V in specific cases. The I-V properties were explained in terms of the DOS and linked to the transmission spectrum in each case. From the obtained results, we can observe that the studied systems have low probability of electrical charge transport in the calculated range, in agreement with the experimental values. These results show that $AlF_3$ could be effectively used as a thin insulating film for electronic heterostructures under voltage ranges between −2.5 to 5 V. Showing as well that even a single molecule might act as an efficient decoupling structure.

## Acknowledgements

The authors acknowledge financial support from the Argentinian institutions Consejo Nacional de Investigaciones Científicas y Técnicas (CONICET), Agencia Nacional de Promoción Científica y Tecnológica (ANPCyT), Universidad Nacional de Entre Ríos (UNER) and Universidad Nacional del Litoral (UNL).

## References

[1] Wander A, Bailey CL, Mukhopadhyay S, Searle BG, Harrison NM. J Mater Chem 2006;16:1906–10.
[2] Bailey CL, Mukhopadhyay S, Wander A, Searle BG, Harrison NM. J Phys Conf Ser 2008;117:1906–10.
[3] Vergara LI, Vidal R, Ferrón J. Appl Surf Sci 2004;229:301.
[4] Ma C, Berta Y, Wang ZL. Solid State Commun 2004;129:681.
[5] Konig R, Scholz G, Scheurell K, Heidemann D, Buchem I, Unger WE, et al. J Fluorine Chem 2010;131:91.
[6] Chen YR, Perebeinos V, Allen PB. Phys Rev B 2004;69:054109.
[7] Chupas P, Ciraolo M, Hanson J, Grey C. J Am Chem Soc 2001;123:1694.
[8] Le Bail A, Calvayrac FJ. J Solid State Chem 2006;179:3159.
[9] Moreno-López JC, Vidal R, Passeggi Jr. MCG, Ferrón J. Phys Rev B 2010;81:075420.
[10] Ruano G, Moreno-López JC, Passeggi Jr. MCG, Vidal R, Ferrón J, Niño MA. Surf Sci 2012;606:573–9.
[11] Daniel P, Bolou A, Rousseau M, Nouet J, Fourquet JL, Leblanc M, et al. J Phys Cond Matter 1990;2:5663.
[12] Navarro JL, Albanesi E, Vidal R, Ferron J. Mat Res Bull 2016;83:615–22.
[13] Horcas I, Fernández R, Gómez-Rodríguez JM, Colchero J, Gómez-Herrero J, Baró AM. Rev Sci Instrum 2007;78:013705.
[14] Ozaki T, Nishio K, Kino H. Phys Rev B 2010;81:035116.
[15] Ozaki T. Phys Rev B 2003;67:155108.
[16] Ozaki T, Kino H. Phys Rev B 2004;69:195113.
[17] Perdew JP, Burke K, Ernzerhof M. Phys Rev Lett 1996;77:3865.
[18] Monkhorst HJ, Pack JD. Phys Rev B 1976;13:5188.
[19] Gomez L, Martin V, Garces J, Ferron J. J Phys D 2014;47:495305.